

Coronagraphic Polarimetry of Disks Around Herbig Ae/Be Stars: Investigating Disk Properties and Dust Grain Growth with HST NICMOS

Marshall D. Perrin (UCLA; mperrin@ucla.edu) Glenn Schneider (U of Arizona), Dean C. Hines (Space Sciences Institute), John P. Wisniewski, (U of Washington), Carol A. Grady (NASA GSFC), and the HST GO-11155 Team

Using the unique capabilities of HST NICMOS, we have obtained 2 μm coronagraphic polarimetry and 1 μm coronagraphic imaging of primordial circumstellar disks around several Herbig Ae stars. These data both clarify disk geometry and reveal distinctly different dust scattering properties around different sources, largely consistent with grain growth to larger sizes around older sources. We here present our coronagraphic images of these disks, and summarize our ongoing analysis and modeling efforts.

Why study dust grain growth in young disks?

Primordial circumstellar disks around young stars dissipate over timescales of a few million years, giving birth to a great diversity of planetary systems. The growth of dust grains in these disks, from sub-micron ISM grains to macroscopic particles to centimeter-sized rocks, is a key part of planet formation processes.

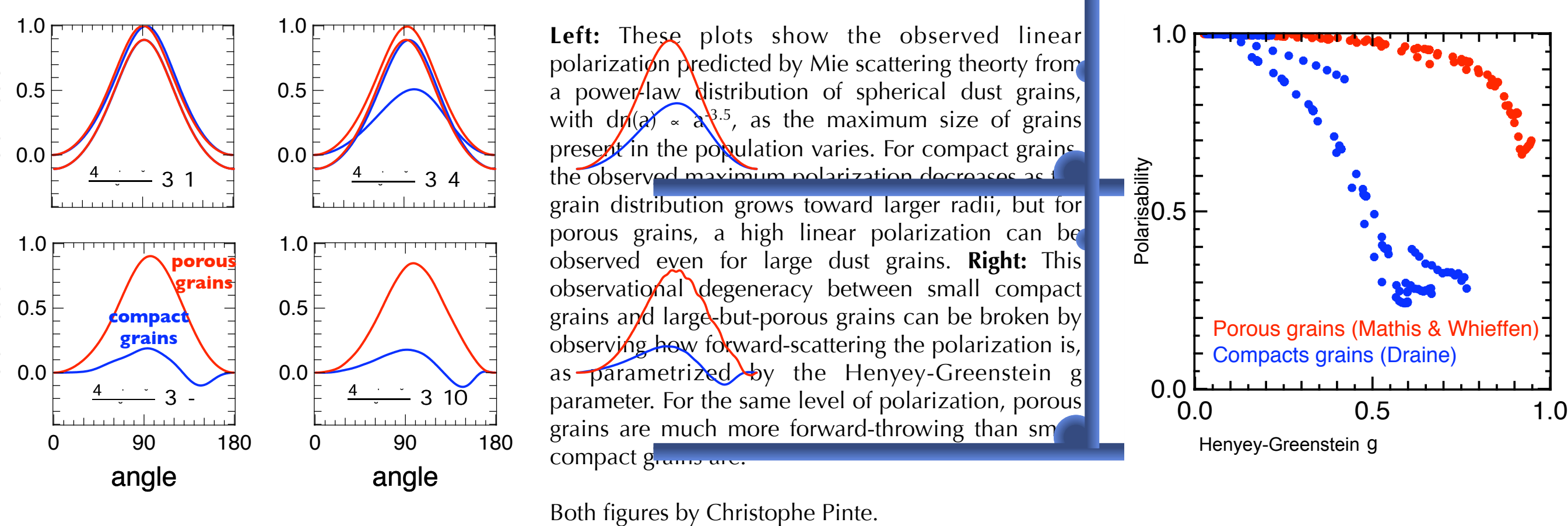
High-contrast resolved imaging of disks lets us study the distribution of grain properties within disks, the timescales over which those properties change, and the physical processes which affect them such as collisional aggregation and fragmentation, vertical settling toward the midplane, and radial migration.

Coronagraphic polarimetry can constrain disk & dust properties

The linear polarization of scattered light depends on the size of the scattering particle, its optical indices and the scattering angle. Thus imaging polarimetry is sensitive to both disk geometry and orientation, and to the dust grain populations within a disk.

Different wavelengths of light probe different depths within the disk and are most sensitive to different grain sizes, roughly proportional to wavelength. Thus *multiwavelength* imaging and polarimetry provides a powerful and sensitive tool to ascertain the size distribution of the sampled grain population.

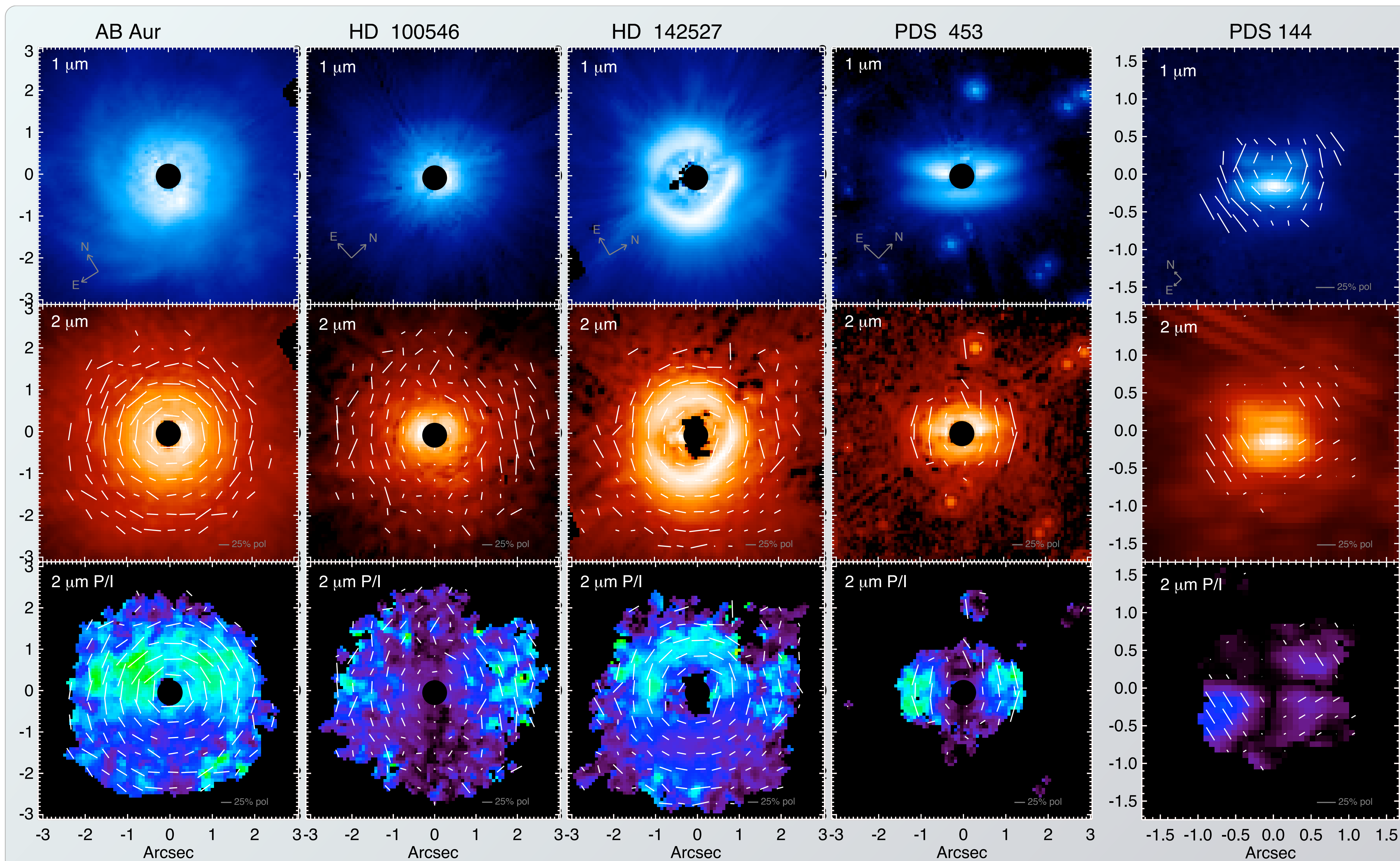
Extracting physical parameters from observations of these optically thick disks requires comparisons with numerical models, such as from Monte Carlo radiative transfer (e.g. Dominik & Dullemond 2003, Pinte et al. 2007, 2008). Obtaining rich multiwavelength datasets merging imaging, polarimetry, and spectroscopy greatly improves the return from such analyses, breaking model degeneracies and allowing tight constraints to be derived (Watson et al. 2007). Studying the complete grain population requires the combination of data across wavelengths ranging from sub-micron to microns up to millimeters and beyond.



NICMOS Polarimetry Observations & Data Reduction

- The NICMOS coronagraph on Hubble remains the best tool for obtaining photometrically accurate and absolutely calibrated high-contrast polarimetry (Hines & Schneider 2006), as needed for comparisons with disk models.
- Previous NICMOS programs have obtained coronagraphic imaging polarimetry of both T Tauri and debris disks (GO 10847, 10852; PIs: Hines & Schneider).
- By obtaining a comparable dataset for selected Herbig Ae/Be stars (young stars of intermediate mass) we will be able to study how disk properties vary with stellar mass, and thereby gain insight into the origins of the disparate planetary systems now observed around low- and intermediate-mass stars.

We followed the recommended observational strategy for NICMOS coronagraphy, obtaining data in two roll angles for each target to allow subtraction of instrumental artifacts. We also observed several unpolarized reference stars for PSF subtraction. Total integration times varied slightly between targets, but are typically ~ 700 s in each of the three POL*L polarizer filters plus ~ 500 s in F110W. We also obtained short (few second) unocculted observations for flux calibration. Starting with the HST pipeline calibrated data products, we performed sky subtraction, bad pixel repair, and PSF subtraction using the IDP3 IDL program. We developed an automated iterative PSF subtraction tool based on IDP3 which identified the optimally matched PSF star for each science orbit, and performed a registered and scaled subtraction to remove the stellar PSF. The polarizer data were then combined using the POLARIZE software to obtain linear polarization (Stokes I, Q, U) images, and the visits were combined using an artifact-masked SNR-weighted mean.



Above: 1 and 2 micron NICMOS coronagraphic imaging and 2 micron linear polarization fraction (P/I) for our targets. Images are shown on a log-like asinh stretch, while polarization fraction is on a linear scale; the 0.3" radius black circle is the region occulted by the NICMOS coronagraph. All targets display the centrosymmetric bulls-eye polarization pattern characteristic of light scattered from a circumstellar disk. The 1 micron (F110W) imaging has higher angular resolution and superior coronagraphic performance, allowing finer details of disk structure to be seen than in the 2 micron polarimetry, but all disks are clearly detected at both wavelengths at high S/N.

TARGETS:

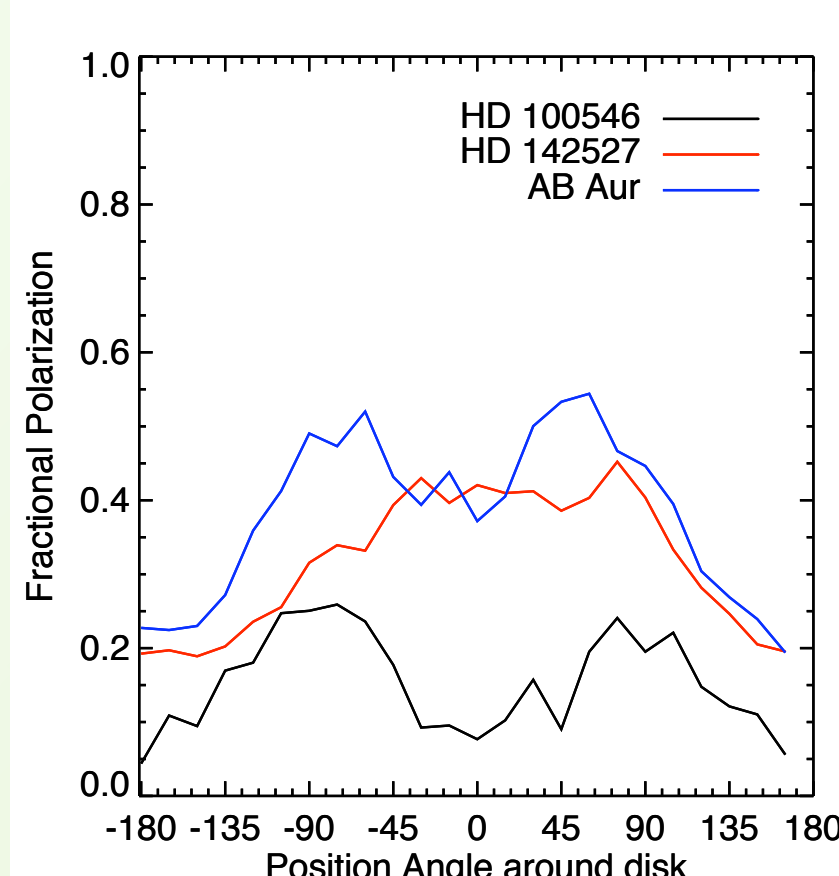
Name	Sp. Type	Dist.	Inclination	V	H	Refs
AB Aur	A1	144	30 ± 5	7.1	5.1	Grady et al. 1999, Oppenheimer 2008
HD 100546	B9	103	50 ± 5	6.7	6.0	Grady et al. 2001, Ardila et al. 2007
HD 142527	F6	140	30 ± 10	8.3	5.7	Fukagawa et al. 2006, Fujiwara et al. 2007
PDS 453	F2	140	75 ± 5	12.9	10.0	Vieira et al. 2003
PDS 144	A2	140?	83 ± 3	14.0	11.4	Vieira et al. 2003, Perrin et al. 2006

Above: For the edge-on PDS 144 disk, we did not need to use the coronagraph, and thus could also obtain 1 micron polarimetry with the NIC1 camera. The observed polarization is clearly lopsided, with the northern corner much less polarized. Not only is this asymmetry seen at both 1 and 2 μm , it perfectly matches the pattern seen in Lick AO polarimetry from 2004. It is a real astrophysical phenomenon, not an observational error!

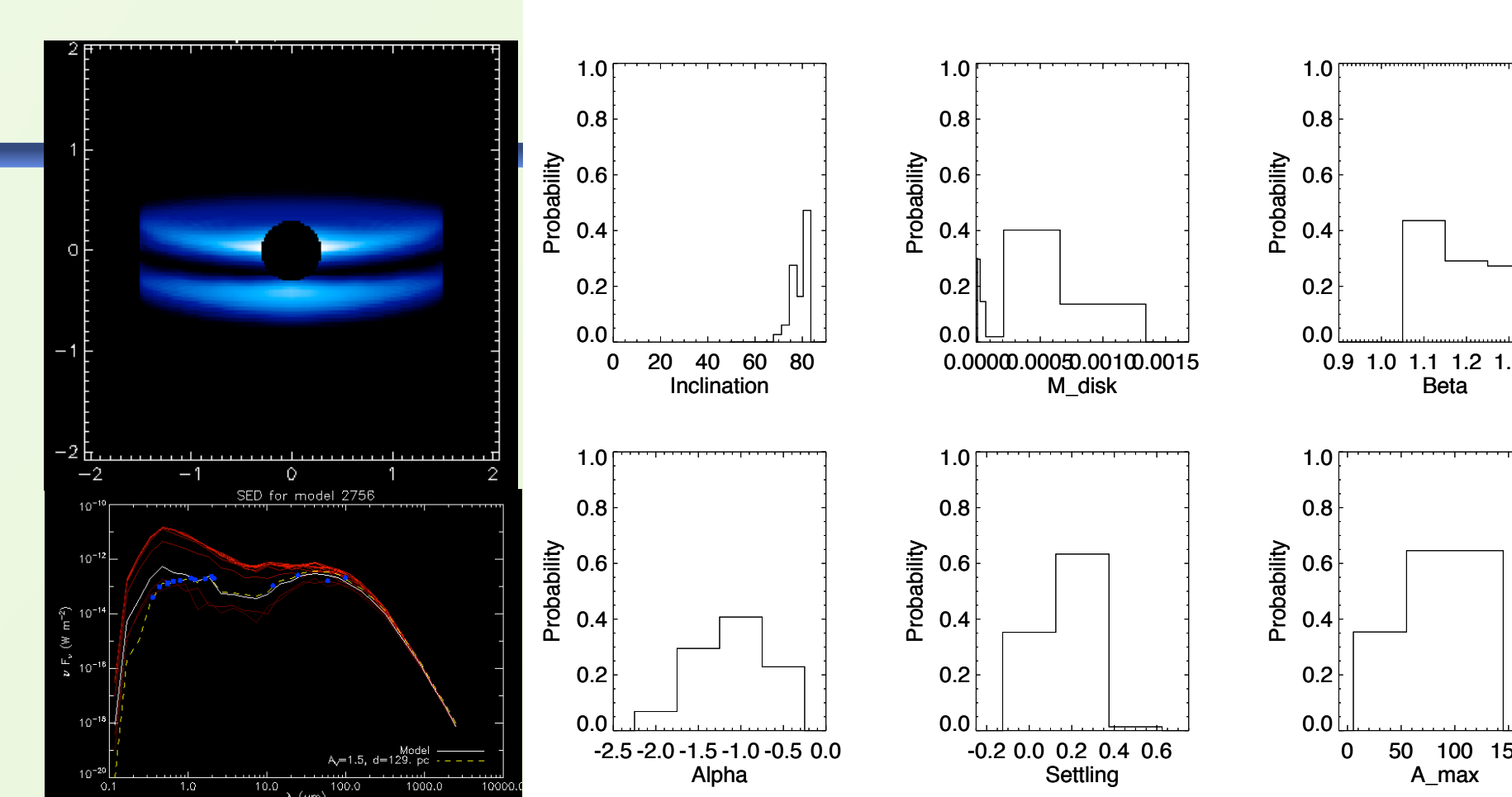
Ongoing Analysis & Modeling

We are in the process of analyzing these data, including measurement of disk properties and extensive comparison with radiative transfer models. We present here only very preliminary results as examples of work in progress.

For the three intermediate-inclination disks, we can measure how the polarization fraction varies azimuthally around the disk, shown below. All three disks show distinctly different polarization patterns. AB Auriga's disk ranges between 20-50% polarized, with the highest polarizations occurring on the rear sides of the disk; this pattern is precisely as predicted based on Mie scattering models for power-law dust distributions, as shown in the inset model figure below right. HD 100546 shows a similar pattern with dual peaks, but with much



lower polarization, suggesting a more evolved, larger grain population is present. This is consistent with the estimated ages of the systems, ~ 3 Myr and ~ 10 Myr respectively. Meanwhile HD 142527 shows high polarization like AB Aur, but the profile has a single broad peak, rather than two shoulders, for reasons yet unknown.



We plan to model each observed system using Monte Carlo radiative transfer disk codes, especially MCFOST (Pinte et al. 2006). This is a computationally demanding problem: Because the phase space of disk models is complex, with many local minima, the most robust approach for global optimization is to compute large grids of models (typically 10^5 - 10^6 models), compare each to the data, and then derive marginal probability distributions for the quantities of interest.

We have developed improved automated tools for this process, following the approach of Pinte et al. 2007. We show above a preliminary best-fit model for PDS 453, which matches well both the observed F110W image and the 0.5-100 μm SED, as well as marginal distributions for various disk parameters. We note these are very early results, so should be considered with caution, but our results thus far indicate both grain growth to large sizes ($\sim 100 \mu\text{m}$) and moderate settling toward the disk midplane have both occurred around PDS 453.

Acknowledgements

Support for this work was provided by NASA through grant number GO-11155 from STScI, which is operated by AURA under NASA contract NAS5-26555. MDP is supported by the NSF Astronomy & Astrophysics Postdoctoral Fellowship Program under grant AST-0702933.

References

- Ardila, D. R., Golimowski, D. A., et al. *AJ*, 665, 2007, 512
 Dominik, C., Dullemond, C. P., et al. *astro-ph*, 2002
 Fujiwara, H., Honda, M., et al. *AJ*, 2006
 Fukagawa, M., Tamura, M., et al. *AJ*, 2006
 Grady, C., Polomski, E., et al. *AJ*, 2001
 Grady, C., Woodgate, B. E., et al. *AJ*, 1999
 Hines, D. C. & Schneider, G. *astro-ph*, 2006
 Oppenheimer, B. R., Brenner, D., et al. *AJ*, 679, 2008, 1574
 Perrin, M. D., Duchêne, G., et al. *AJ*, 645, 2006, 1272
 Pinte, C., Fouchet, L., et al. *arXiv*, 2007
 Pinte, C., Padgett, D. L., et al. *A&A*, 489, 2008, 633
 Vieira, S. L. A., Corradi, W. J. B., et al. *AJ*, 2003
 Watson, A. M., Stapelfeldt, K. R., et al. *PPV*, 2007, 523